Hindawi
Geofluids
Volume 2021, Article ID 5593601, 13 pages
https://doi.org/10.1155/2021/5593601

Research Article

Research on Full-Section Anchor Cable and C-Shaped Tube Support System of Deep Layer Roadway

Renliang Shan, Shupeng Zhang, Pengcheng Huang, and Weijun Liu

School of Mechanics and Civil Engineering, China University of Mining and Technology-Beijing, Beijing, China

Correspondence should be addressed to Shupeng Zhang; 782640988@qq.com

Received 5 January 2021; Revised 29 January 2021; Accepted 1 February 2021; Published 16 February 2021

Academic Editor: Feng Xiong

Deep roadway deformation due to soft rock, rock dip, and horizontal tectonic stress is uneven and asymmetrical primarily in large loose zones. Traditional anchor support is influenced by the yield strength and shear strength of the anchors and has a limited prestress capacity or shear resistance. When the roadway roof is laminated rock or when the roadway passes through layered rock or rock interfaces, interlayer sliding commonly occurs, which can easily lead to anchor cables being sheared off. The tape tunnel in the Zhengling Mine passes through several rock strata and requires anchors to achieve a high shear resistance and prestress. To solve these problems, an anchor cable and C-shaped tube that can bear lateral shear forces were developed, and a full-section anchor cable and C-shaped tube support system were created based on extruded arch theory. Numerical results from FLAC^{3D} show that the new scheme effectively controls surface convergence and plastic zone extension. Field tests have demonstrated that the amount of surface displacement was at least 42% smaller in the new support scheme. The extruded arch formed by the highly prestressed anchor cable and concrete spray layer can effectively control the bulking load within the loose zone, and the ACC effectively resists interlayer shear.

1. Introduction

Coal-bearing strata are common stratified formations, where roof separation and sliding between rock strata are easily observed during roadway excavation [1, 2]. With increasing mining depth, the frequency of roof separation and interlayer sliding significantly increased due to the rock dip, soft rock, and high ground stress, especially the high level of tectonic stress. Deep roadway surrounding rocks exhibit large loose zones and significant asymmetrical large deformation [3, 4]. Statistics show that after roadway excavation and unloading, the vertical deflection of the roof and the lateral interlayer shear slip cause dangerous stresses on the anchor cables. Except for the anchor cables arranged in the center of the roof, the remaining anchor cables are primarily under the combined action of axial tension and lateral shear. Anchor cables need to resist not only the axial tension generated by the deformation of the surrounding rock but also the lateral shear forces caused by interlayer sliding, resulting in not only tensile failures but also a large number of shear failures. Due to the special characteristics of the anchor cable structure and its high strength, testing the shear mechanical properties in the field is difficult, and, at present, the shear properties of anchor cables are primarily studied using indoor shear tests. In laboratory studies of bolted rock joint shear behavior, in situ conditions cannot be fully replicated primarily due to rock/concrete sample dimensions [5].

Numerous studies have been conducted on rock bolts and anchor cables. When a pretensioned rock bolt is subjected to a shear load, the maximum shear force can reach up to 80% of the rock bolt tensile capacity [6, 7]. Compared with end-bolt anchoring, full-length bolt anchoring provided a superior anchoring effect by increasing the strength and shear-bearing capacity of the rock [8]. Grouting the joint improved the force condition of the bolt, increased bolt yield displacement, and coordinated the deformation of the grouting body and bolt, thereby improving joint shear strength [9].

Pretightening force has a significant effect on the anchor cable and the anchored joint. It has been experimentally demonstrated that the overall stiffness of an anchor cable increases as the pretightening force increases [10]. In all cases, increasing the strength of the surrounding rock and

the pretightening force of the anchor cables enhances the shear strength of the jointed surrounding rock, and the shear strength of the pretightened anchor cables is much greater than the shear strength of the surrounding rock [11–13]. The pretightening force also affects the stress-strain curve of the anchored joint rock [14]. Increasing the pretension load decreased the peak shear load of cable bolts [15, 16]. As the anchor cable pretightening force increases, the initial shear stiffness of the joint increases [17–19]. When the pretightening force is increased, the prestress field formed in the surrounding rock expands and the shear stiffness of the anchor system increases significantly. However, when the pretightening force is too large, the anchor bolts tend to yield prematurely. The pretightening force should generally not exceed 50% of the bolt yield load [20], which limits the positive effect of prestressing the jointed rock. Anchor cables are characterized by a high pretightening force, low elongation, and relatively low shear strength, which makes them susceptible to failure when resisting shear loads. Therefore, it is imperative to develop a support component with high shear capacity and high pretightening force.

In theory, the surrounding rock excavation process will produce fragmentation and expansion deformation, which will produce a crushing and expansion load that is even larger than the self-weight of the rock. The crushing and expansion load is the main load on the surrounding rock support system. Most deep roadways have large loose zones with radii greater than 150 cm characterized by extruded arch theory [21]. Different from the combined arch theory, extruded arch theory emphasizes maintaining the integrity of the extruded arch by protecting the surrounding rock from falling blocks using a reinforcement mesh, concrete spray layer, and other surface protection components [22].

In this study, a shear resistant anchor cable with a high pretightening force and high shear resistance was developed based on anchor cables and shear load distribution in deep roadways [23]. A full-section anchor cable and C-shaped tube support was constructed based on the extruded arch theory, and an ACC optimization scheme was proposed and tested in the field.

2. Project Profile

The starting point of the new section of the tape tunnel in Zhengling Mine is located below the bottom of the 2# coal seam and has a design length of 820 m. The tunnel is dug upwards at a +15° slope. The coal and rock strata have an average dip of 10° and maximum dip of 14°. The starting point of the new section is 520 m deep. The surrounding rocks are primarily mudstone, sandy mudstone, thin coal stratum, and poorly cemented fine sandstone. The strength of the contact surface between the layers is low. The tunnel has straight walls and semicircular arch section and is 4700 mm wide and 3850 mm high.

The original support scheme of the tape tunnel uses a combination of anchor bolts, anchor cables, steel reinforced ladder beams, steel reinforced mesh, and concrete spray layer (Figure 1). Two rows of anchor bolts are arranged each with 13 anchor bolts, with 800 mm between two anchor bolts in the same row. Anchor cables are arranged between the two rows of anchor bolts, with 1600 mm between two adjacent rows of anchor cables. Anchor bolts in the same row are connected by reinforcement ladder beams, and the reinforcement mesh is pressed against the surrounding rock by the reinforcement ladder beams. The roadway surface is sprayed with a 150 mm thick layer of C25 concrete. The anchor bolts have a torque of no less than 190 N·m, and the anchor cables have a pretightening force of no less than 150 kN.

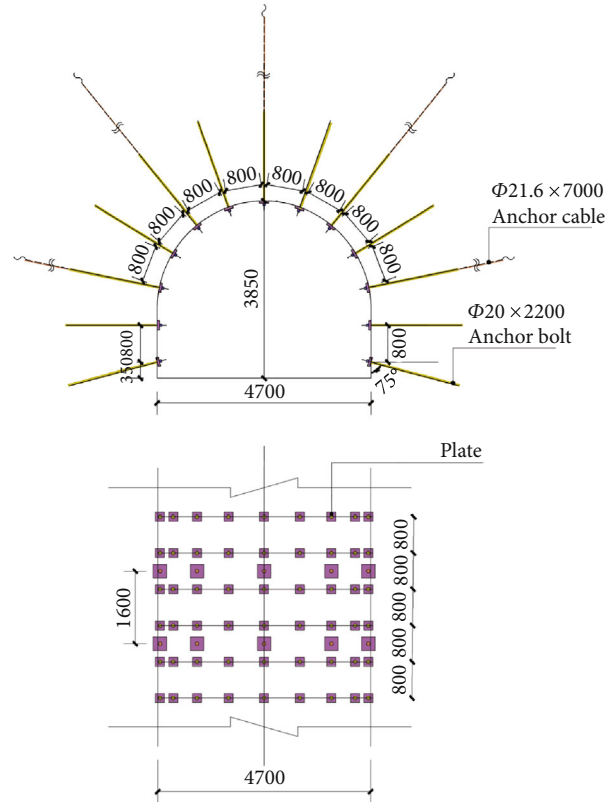

Figure 1: Cross-sectional sketch of the original support scheme.

2.1. Analysis of Surrounding Rock Failure Characteristics. The following deformation and failure characteristics of the surrounding rock in the roadway were identified: (1) the overall roadway deformation is large and primarily concentrated in the roof and shoulders; (2) the roadway shows significant asymmetrical deformation under high in situ stress and high horizontal tectonic stress; (3) the right shoulder of the vault is the first to undergo deformation after excavation due to the dip in the rock layer, followed by the left shoulder and the left side; and (4) rock sliding is evident, and the anchor cables were sheared off in multiple locations.

Large deformations were found in the roof and shoulder of the vault, the surrounding rock on the left shoulder was extruded under high stress and the tunnel was unevenly deformed (Figure 2(a)). Some of the anchor bolts in the roof failed, and the shoulder anchor cables were sheared off (Figures 2(b) and 2(c)). Although measures were taken to replenish the anchor cables and sprayed concrete, the replenished concrete was easily dislodged (Figure 2(d)), making

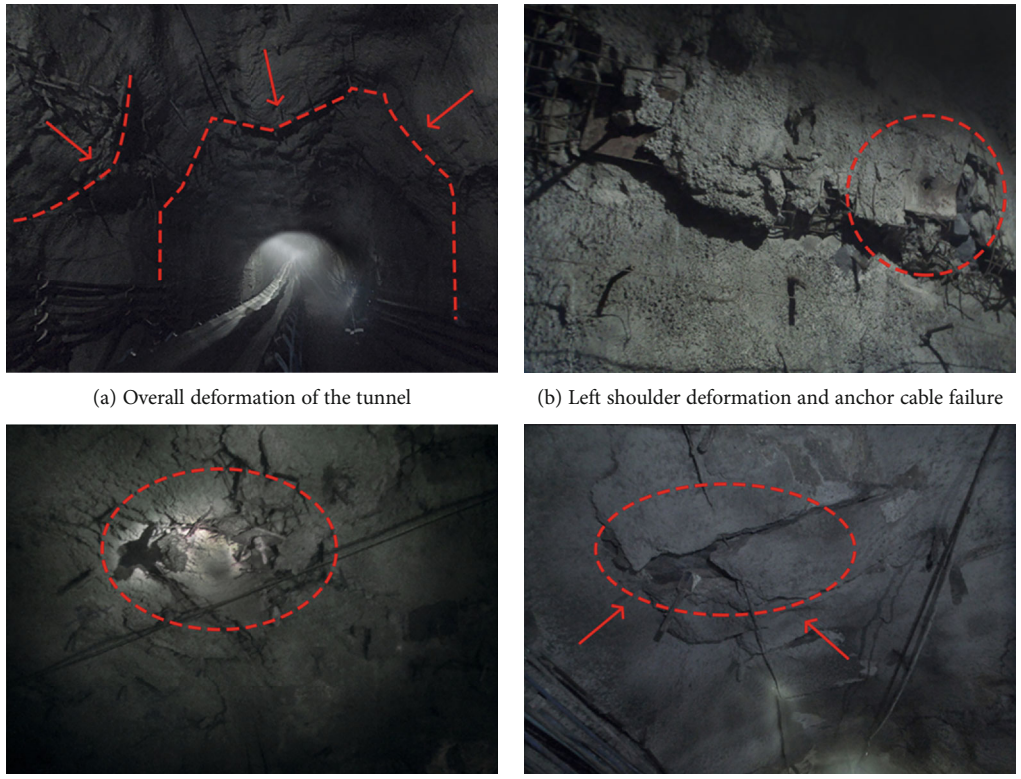

(a) Overall deformation of the tunnel

(b) Left shoulder deformation and anchor cable failure

(c) Failure of roof anchor cables

(d) Concrete falling out of the roof

Figure 2: Roadway deformation and failure of anchor cables diagram.

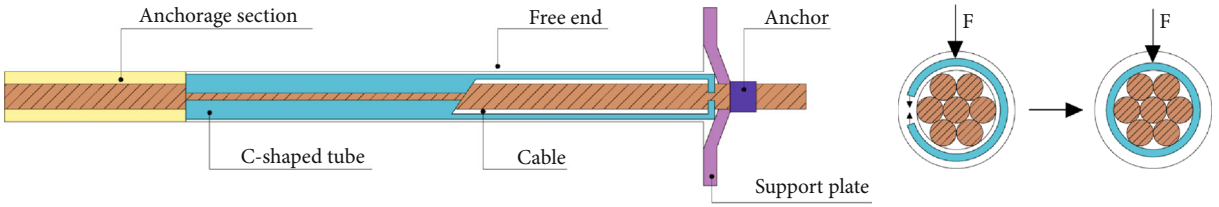

(a) Structural drawing of an ACC

(b) ACC action mechanism diagram

Figure 3: ACC structural and action mechanism diagram.

restraining the development of the tunnel surrounding rock deformation difficult.

The tape tunneling process passes through several rock formations. The shear slip at the interface between rock layers and fracture surfaces in the surrounding rock within a certain range from the tunnel surface poses great difficulties when supporting the surrounding rock. Due to the large burial depth of the tape tunnel, the high self-weight stress, and the superposition of horizontal tectonic stress, the interlayer shear stress is high.

The maximum dip angle of the rock layers is 14°. After the tunnel is excavated, the deformation of the surrounding rock in different parts of the tunnel occurs variability, and the support structure is prone to uneven loading and low coupling with the surrounding rocks. The roof is susceptible to the formation of tensile fracture zones when subjected to tensile stresses, resulting in roof surface rock instability in the direction perpendicular to the layers. Following deformation of the roof rock, interlayer sliding is induced in the shoulder causing further fracturing of the surrounding rock. The fractured surrounding rock at the shoulder of the roadway is then extruded due to the high horizontal stress. Ordinary anchor cables have poor shear resistance and are easily sheared off, causing partial failure of the support structure, which results in large local deformation and reduces the ability of the support structure to transfer stress to the surrounding rock, thus inducing an overall catastrophic destabilization of the roadway.

3. Full-Section ACC Support System

3.1. Introduction to ACC. The ACC is a type of prestressing anchor cable with a high transverse shear capacity at the free end [24] (Figures 3 and 4). ACC consists of C-shaped tubes

Figure 4: Image of C-shaped tubes.

and regular anchor cable parts such as anchor cable, capsule resin, locking devices, and plate. The anchor cable passes through the C-shaped tube and is anchored in the surrounding rock. The C-shaped tube is similar in construction to a pipe slit anchor with an indented head end and a full slit along the longitudinal axis, wrapping the free end of the anchor cable.

The C-shaped tube length is slightly smaller than the free end of the anchor cable, ensuring that the anchor cable prestress can be diffused into the surrounding rock. When the free end of the shear-resistant anchor cable is subjected to lateral shear, the C-shaped tube is gradually compressed and deformed until the free end of the anchor cable is wrapped, enhancing the shear resistance of the free end of the anchor cable (Figure 3(b)).

3.2. Shear Load Sources in Roadways. Rock is typically an inhomogeneous medium with a large number of internal structural surfaces. After roadway excavation, under the action of the in situ stress and secondary stress, a loose zone is created. The ruptured surrounding rocks within the loose zone tend to slip along the rupture surface. The closer to the roadway surface, the more significant the crack expansion is and the higher the rupture degree. Shear expansion deformation resulting from shear sliding along the rupture face can lead to increased shear forces on the anchor cable within the loose zone.

When the roadway roof is stratified or passes through different rock stratums, the strength of the contact surface between the rock strata is uneven. Under high in situ stress, the part of the interlayer with low cohesion fails first, prompting the part with higher cohesion to break down as well and making the interlayer contact more susceptible to interlayer sliding. When the tunnel passes through alternating hard and soft rock layers, the various water absorption and softening characteristics also affect surrounding rock deformation. Some rock layers, such as mudstone, swell after absorbing water, causing their strength to decrease significantly. The tunnel is first damaged in the soft rock, where extrusion and deformation occur due to the high in situ stress. The dip of the rock layer can exacerbate both extrusion and deformation, exposing the anchor cables to higher shear loads at the rock interface between the roof and shoulder.

3.3. Full-Section ACC Support System. A full-section ACC support system is proposed based on the theory of large loosened zone extrusion arches in deep roadway and the associated shear load distribution characteristics, combined with the structural characteristics of high prestressing and high shear resistance at the free end of ACCs. In the support design, the full section of the roadway is supported using ACCs, W-shaped steel strips connecting the ACCs, and pressing the reinforcement mesh onto the roadway surface. Tunnels with a loose zone greater than 150 cm require shotcrete on the roadway surface with a concrete strength of no less than C25.

Selection of the right length of anchor cable and C-tube is key to the design. In general, the anchor cable length depends on the anchorage section length, free section length, and exposed length of the anchor cable. The C-shaped tube length can be taken as the thickness of the loose zone, and the free end length should be slightly greater than the C-shaped tube length. According to the extruded arch theory, the extruded arch thickness b is determined by

$$b = \frac{L \times \tan \alpha - a}{\tan \alpha}, \tag{1}$$

where L is the anchor cable length, α is the control angle of the anchor cable on the fractured rock (generally 45 degrees), and a is the anchor cable spacing. As can be seen from Equation (1), the thickness of the extruded arch increases with increasing anchor cable length and increases with decreasing anchor cable spacing.

Determination of the extruded arch thickness is crucial to the design of the anchor length and spacing. At this point, it is possible to draw on loose zone suspension theory by multiplying the anchor loose zone thickness by a safety factor as the extruded arch thickness. The loose zone thickness can be determined accurately by means of borehole peeping, ultrasound, and rock resistivity [20].

If the thickness of the extruded arch is equal to the thickness of the loose zone, the shortest anchor cable length is the thickness of the loose zone plus the anchor cable spacing. Anchor cables that require suspension should be extended reach a stable rock layer. The C-shaped tube length (free section length) should be extended where the top and shoulder of the roadway are close to the rock interface and where anchor cables are required to resist possible interlayer sliding.

When interlayer sliding may occur near the roadway, the roof and shoulder C-shaped tube lengths are determined by the thickness of the loose zone, the rock intersection, and the distance from the roadway surface, as determined by

$$L_t = \max \{L_c, L_d + L_s\}, \tag{2}$$

where L_c is the length of the C-shaped pipe, L_b is the thickness of the loose zone, L_d is the length of the anchor cable from the surface position of the roadway to the rock interface, and L_s is the reserved safety length, which is taken as more than three times the diameter of the anchor cable hole (generally 100 mm).

3.4. Full-Section ACC Support Mechanism. The full-section ACC support system is primarily aimed at medium and large loose zone exhibited in deep roadways, controlling the deformation of the surrounding rock in the loose zone through the extruded arch formed by the anchor cables, reinforcement mesh, and concrete spray layer. The support system combines the distribution of shear loads in the roadway and the failure condition of the anchor cables to determine a reasonable C-shaped tube length and give full play to the high shear strength and high prestress of the ACC, specifically the following points:

(1) Excavation of the surrounding rock will result in fragmentation and expansion, which will generate fragmentation and expansion loads even greater than the weight of the rock mass. The fragmentation and expansion loads are the primary axial loads on the ACC support. The fracture expansion force and deformation generated by the fracture surface slipping under stress concentration within the loose zone as well as the interlayer sliding at the interface between the rock layers in the roof are primary lateral load on the ACC support

(2) The ability of the ACC to support shear loads is composed of two parts, the high pretightening force and the shear stiffness provided by the C-shaped tube. The C-shaped tube outer wall is closer to the hole wall than the free end of the normal anchor, making the C-shaped tube fit snugly within the surrounding rock earlier after the fractured surrounding rock has been deformed by fragmentation and expansion. The ACC can play a similar role to the full-length bolt in terms of shear resistance in the early stage of shear deformation. The high pretightening force enhances the axial tensile stress of the anchor cable, which in turn increases the shear strength of the jointed surrounding rock

(3) According to the extruded arch theory of large loose zones, the surrounding rock within the loose zone will form a conical extrusion zone under the extrusion of a single ACC. After multiple ACCs are reasonably arranged along the roadway surface, the conical extrusion zones overlap with each other to form a continuous extrusion zone of a certain thickness. As long as the roadway surface is reinforced using reinforcement mesh, shotcrete, and other surface protection measures to limit its extrusion from falling blocks, the rock mass inside the extrusion zone, regardless of whether it is fragmented or not, will be in a three-way stressed state which significantly increases its mechanical properties and effectively enhances roadway stability

(4) For stratified rock layers or dipping rock joints, after roadway excavation and unloading, separation of the roof from vertical deflection and lateral interlayer shear slip is the primary cause of anchor cable failure,

Table 1: Measured results of the in-situ rock stress test.

Classification	Stress (MPa)	Dip (°)	Azimuth (°)
σ_1	36.15	20.6°	258.55°
σ_2	17.08	9.8°	-15.18°
σ_3	14.19	-66°	230.84°
$\sigma_{(h,max)}$	32.77		
$\sigma_{(h,min)}$	18.27		
σ_v	16.56		

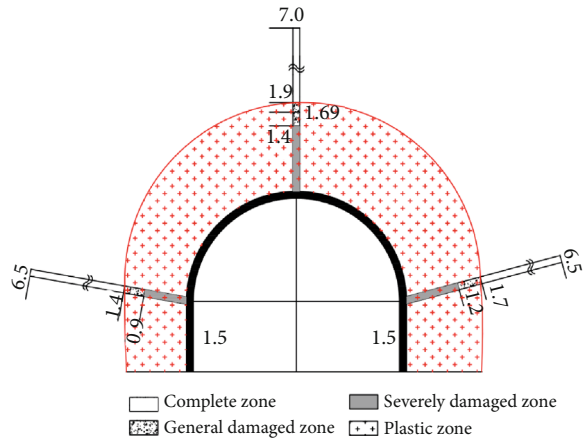

Figure 5: Map of the plastic zone of the surrounding rock.

and anchor cables primarily work under the combined action of axial tension and lateral shear. For anchor cables under combined tension and shear, the relationship is satisfied at the cable breakage location [25]

$$\left(\frac{N_o}{N_f}\right)^2 + \left(\frac{Q_o}{Q_f}\right)^2 = 1, \tag{3}$$

where N_o is the tensile force on breaking of the cable (kN); Q_o is the shear force on the cable at failure (kN); N_f is the ultimate tensile strength of the cable (kN); and Q_f is the ultimate shear strength of the cable (kN). From Equation (3), the shear failure force of the anchor cable decreases with increasing pretightening force. Therefore, ACC provides shear resistance at the free end, resolving the conflict between pretightening force and shear resistance

(5) ACCs need to be used in association with W-shaped steel strips and reinforcement mesh. W-shaped steel strips have high stiffness and can balance the internal forces of the support structure, protecting the surface by preventing stress concentrations and anchor cables fracture. Reinforcement

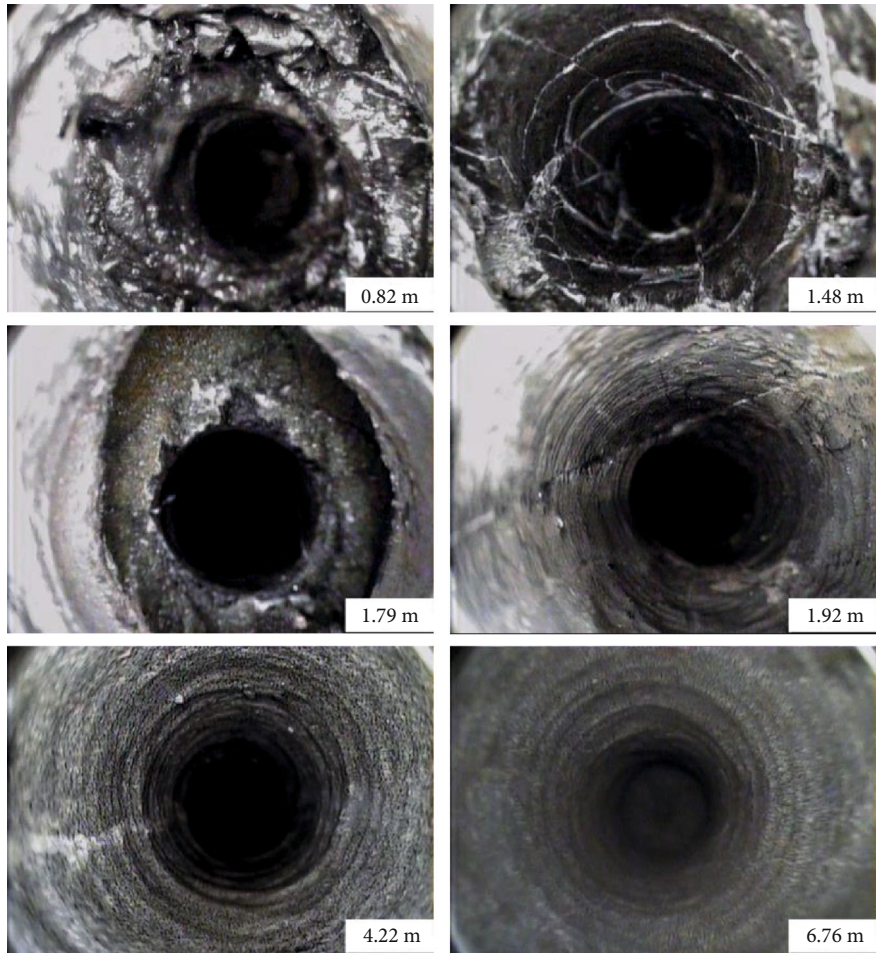

Figure 6: Representative peephole result map.

mesh is a necessary surface protection component to prevent the extrusion of the broken surrounding rock and to ensure the integrity of the extruded arch. In the case of large loose zones, the shotcrete with a concrete strength of no less than C25 should be applied the roadway surface

4. ACC Optimization Scheme for the Tape Tunnel

4.1. In Situ Rock Stress Measurement. To determine the in situ stress distribution characteristics in the Zhengling Mine, a chamber was tested in the original section of the tape tunnel at a burial depth of -710 m. A modified CSIRO hollow inclusion strain gauge was drilled at a depth of 8.5 m at a horizontal inclination of 10 degrees in both sides of the chamber. The main body is a hollow cylinder made of epoxy resin with three resistive strain flowers embedded in the middle at equal intervals along the circumference. Each strain flower consists of four strain gauges, for a total of 12 strain gauges. Based on the measured strain values in the 12 directions on the surface of the small hole, the three-dimensional stress state at the measurement point can be calculated using the following equation:

$$\begin{aligned}
\varepsilon_\theta &= \frac{1}{E}\left\{\left(\sigma_x+\sigma_y\right)k_1+2\left(1-\upsilon^2\right)\right.\\
&\quad\left.\cdot\left[\left(\sigma_y-\sigma_x\right)\cos 2\theta-2\tau_{xy}\sin 2\theta\right]k_2-\upsilon\sigma_z k_4\right\},\\
\varepsilon_z &= \frac{1}{E}\left[\sigma_z-\upsilon\left(\sigma_x+\sigma_y\right)\right],\\
\gamma_{\theta Z} &= \frac{4}{E}(1+\upsilon)\left(\tau_{yz}\cos\theta-\tau_{zx}\sin\theta\right)k_3,\\
E &= \frac{K(p_0/\varepsilon_\theta)R^2}{\left(R^2-r^2\right)},\\
\upsilon &= \frac{\varepsilon_\theta}{\varepsilon_z},
\end{aligned} \tag{4}$$

where $\varepsilon_\theta, \varepsilon_z$, and $\gamma_{\theta Z}$ are the circumferential, axial, and shear strains measured in the hollow inclusions, respectively; σ_x, σ_y, σ_z, τ_{xy}, τ_{yz}, and τ_{zx} are the six components of the three-dimensional stress at the measurement point located in

the three-dimensional right-angle coordinate system OXYZ, from which the magnitude and direction of the three principal stresses σ_1, σ_2, and σ_3 can be determined; and k_1, k_2, k_3, and k_4 are four correction factors, to correct the effects caused by the strain gauges in the hollow inclusion strain gauge not being directly attached to the hole wall [26].

E and υ are the elastic modulus and Poisson's ratio of the core; K is the correction coefficient; p_o is the confining pressure; R is the outer diameter of the core; and r is the inner diameter of the core hole. Results of the in situ stress tests are shown in Table 1.

The results of the in situ stress test at -710 m show the following: (1) the maximum principal stress σ_1 in the stress field is inclined at 20.6° indicating that the ground stress field in this mine is dominated by horizontal stresses rather than by vertical stresses. (2) The maximum horizontal principal stress $\sigma_{(h,max)}$ is 1.79 times the vertical stress σ_v, indicating that the roadway deformation in this area is more influenced by horizontal stresses. (3) The vertical stress σ_v is slightly less than the average weight of the overlying rock layer per unit area, which may be related to the coal mine being located within a loess plateau with a thicker upper loess layer. (4) The maximum principal stress trends SW78° and is inclined at 12° to the tunnel. When the maximum principal stress is between 0° and 20° with the angle of the roadway, the two sides of the roadway bear greater surrounding rock stress than the roof and floor, and the two sides of the support should be strengthened when designing the support structure.

4.2. Analysis of the Distribution of Plastic Zones. To explore the depth of the loose zone around the roadway, a TS-C1201 drill hole imager was used to analyze the two sides and the roadway roof by drilling holes in 6.5-7 m deep peepholes. The area of destruction within the surrounding rock is deep, and the depth of damage to the surrounding rock is uneven. Separation was observed in the roof at 1.69 m deep and was absent in the sides of the tunnel. The surrounding rock is highly fragmented up to 1.4 m above the roof, and the hole walls are primarily fragmented. The surrounding rock is relatively fragmented at 1.4-1.9 m. The hole walls are primarily fractured and jointed, with small fragments. Beyond 1.9 m, the rock is largely intact with localized joints.

The peephole height in the side is 1.5 m, with an average angle of 10°-15° relative to the horizontal. The right side is severely damaged to a depth of 1.2 m, and the rock is relatively intact beyond 1.7 m. The left side is severely damaged to a depth of 1.1 m, and the rock is relatively intact beyond 1.4 m (Figure 5).

The right side of the roadway has a larger depth of destruction than the left side, showing a clear asymmetry, and the roof loose zone is larger than that of the sides. The roadway is surrounded by a large loose zone, with low strength at the rock interface and separation, which is prone to interlayer sliding and extrusion deformation of soft rock caused by high stress. The results of the peephole in the roof are shown in Figure 6.

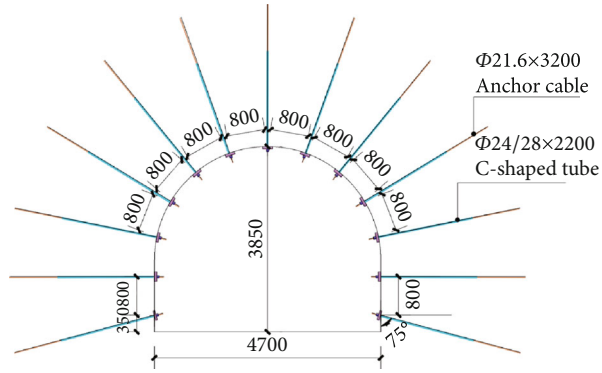

Figure 7: Schematic diagram of the ACC support scheme.

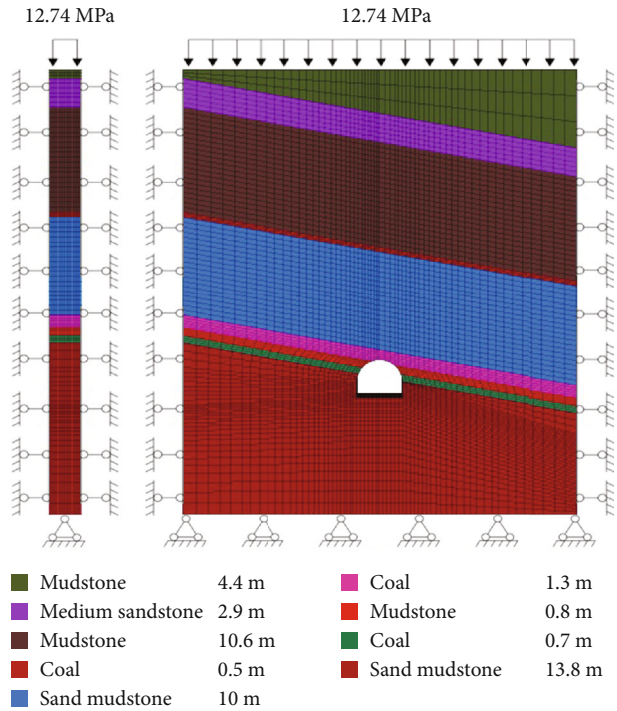

Figure 8: Diagram of the numerical model and boundary conditions.

4.3. Full-Section ACC Support Scheme. The full-section ACC support scheme uses a combination of ACC, reinforced ladder beams, reinforced mesh, and shotcrete. Based on the peephole results, a maximum thickness of 1.9 m was obtained for the loose zone, and a C-tube length of 2 m was selected. When the anchor cables are 3000 mm long and 800 mm apart in the surrounding rock, the extruded arch thickness is 2200 mm according to Equation (4), which is 0.3 m greater than the maximum loose zone thickness. The anchor cables have an exposed length of 200 mm; therefore, it is reasonable to choose a C-shaped tube length of 2 m and an anchor cable length of 3.2 m (Figure 7).

The ACCs are all composed of anchor cables 21.6 mm in diameter and 3200 mm in length and C-shaped tubes 28 mm in outer diameter, 24 mm in inner diameter, and 2000 mm in length.

Table 2: The surrounding rock parameters of each layer.

Stratum	Density (kg/m^3)	Bulk modulus (GPa)	Shear modulus (GPa)	Cohesion (MPa)	Friction angle (°)	Tensile strength (MPa)
Coal	1700	3.1	1.8	0.7	25	0.8
Mudstone	2520	4.1	2.3	1.2	30	1.3
Sandy mudstone	2500	5.5	3	2	33	0.8
Medium sandstone	2650	6	3.6	3	35	2.1

Table 3: Pile unit-related parameters.

Type	emod (GPa)	nu	xcarea (mm^2)	per (mm)	cs_sk (MPa)	cs_scoh (MN/m)	cs_nk (MPa)	cs_ncoh (MN/m)	cs_sfric (MPa)
Pile	200	0.3	4.02*e*4	100	13	13	13	0	25

For each row of 13 ACCs, the distance between two ACCs in the same row is 800 mm, and the spacing between two rows of ACCs is 800 mm. The ACCs in the same row are connected by reinforcement ladder beams, the reinforcement mesh is pressed on the surrounding rock by the reinforcement ladder beams, and the roadway surface is sprayed with 150 mm thick layer of C25 concrete. The anchor cable preload is no less than 200 kN.

5. Numerical Simulation and Analysis of Results

The tape tunnel passes through several rock layers during excavation. For the working conditions when passing through the 2# coal seam, numerical models are built using FLAC^{3D} to compare the original scheme and the full-section ACC support scheme (Figure 8). The model is 40 m long, 3.2 m wide, and 45 m high, with a fixed lower boundary. The other model boundaries are constrained by normal displacement boundaries.

Based on the burial depth, the upper part of the model compensates for a vertical mean surface load of 12.74 MPa. Based on the results of the in situ rock stress test, the horizontal stress is taken as 1.79 times the vertical stress, resulting in a horizontal stress of 22.80 MPa. The Mohr-Coulomb model is used for the numerical simulations, and the ACCs use cable units for the anchor cables as well as shear-resistant pile units for the C-shaped tubes. The beam unit is used for the reinforced ladder beams, and the shell unit is used for the concrete (Tables 2–4).

Table 4: Support member parameters.

Type	Anchor cable	Bolt	Beam	Shell
Diameter (mm)	21.6	20		
xcarea (mm^2)	366	380	307.7	
emod (GPa)	195	200	200	26
Breaking load (KN)	540	216		
gr_per (mm)	100	100		
gr_k/(MN/m/m)	17.5	17.5		
gr_coh (MN/m)	0.44	0.44		
nu			0.3	0.25

5.1. Displacement Analysis. The horizontal and vertical displacements for the two support schemes are shown in Figure 9.

In the original scheme, the area with larger horizontal displacement on the left side is primarily concentrated at the side and shoulder, and the stress distribution range is significantly larger on the right side. The deformation of the right side is larger and primarily concentrated at the connection between the side and the shoulder. It is assumed that the difference between the maximum horizontal displacements of the two side positions divided by the smaller value is the degree of inhomogeneity. Then, the maximum horizontal displacement of the left side is 3.59 mm and the right side reaches 5.07 mm, with a relative difference of 41.23%. The maximum amount of roof sinking is 10.9 mm, and the maximum amount of floor dropsy is 8.29 mm.

In the ACC support scheme, the horizontal displacement is primarily concentrated in the two sides. The maximum horizontal displacement of the left side is 3.17 mm, and the maximum horizontal displacement of the right side is 3.78 mm. The relative difference between the two sides is 19.24%, and the distribution range is more symmetrical. The maximum roof sinkage is 8.92 mm, and the maximum floor heave is 8.06 mm.

Compared with the original support scheme, the ACC support scheme replaces the anchor bolts with 3.2 m long short anchor cables and eliminates the five long anchor cables in each of the two rows in the roof. The deformation of the two sides is reduced by 1.17 mm compared to the original scheme, an optimization of 19.75%, and the relative difference is reduced by 21.99%. Roof sinking is reduced by 1.98 mm, an optimization of 18.16%. The difference of the floor dropsy is not significant, only 2.8%.

The ACC support schemes have a more even deformation volume and distribution range, indicating that the full-section ACC support structure better couples with the surrounding rock, primarily because the high prestressing force of the ACC support scheme enables the three-

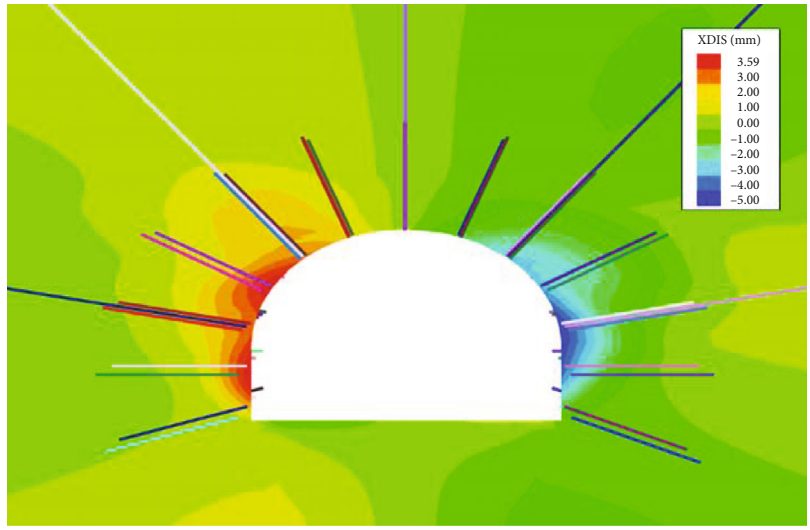

(a) Horizontal displacement of the original scheme

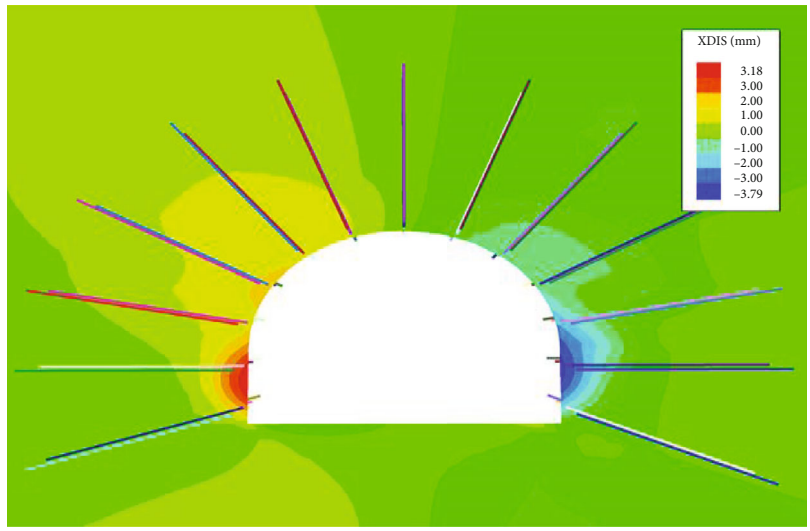

(b) Horizontal displacement of the ACC scheme

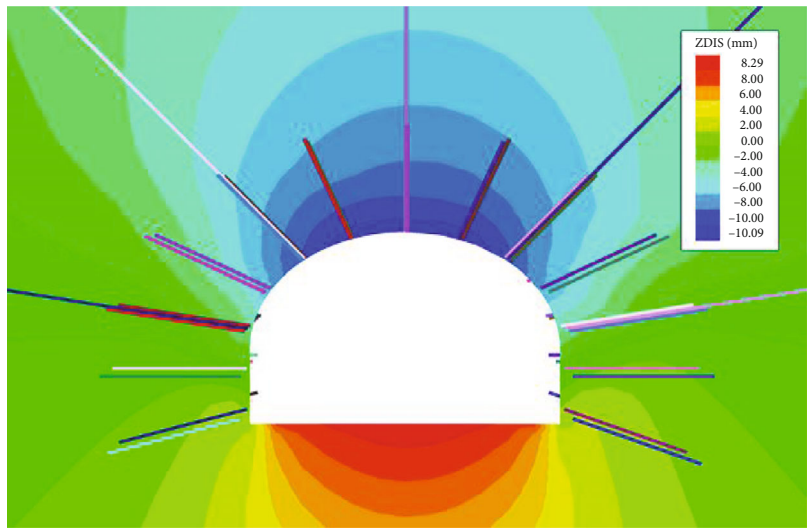

(c) Vertical displacement of the original scheme

Figure 9: Continued.

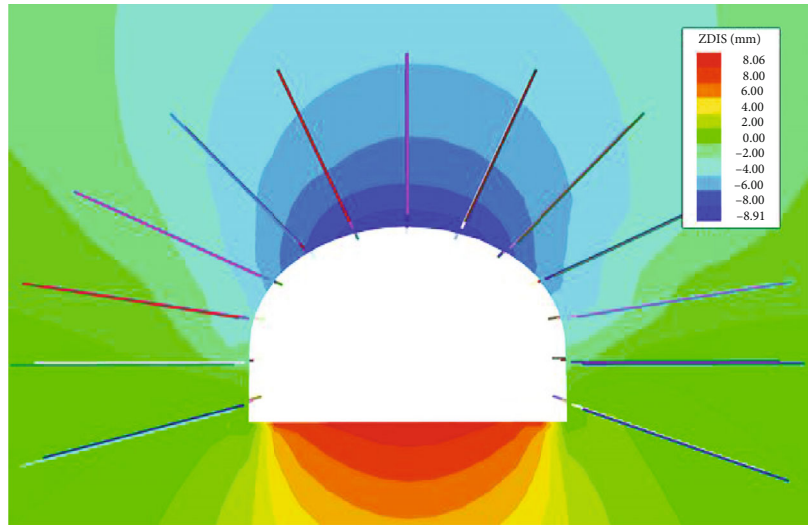

(d) Vertical displacement of the ACC scheme

Figure 9: Displacement cloud diagrams for the two support schemes.

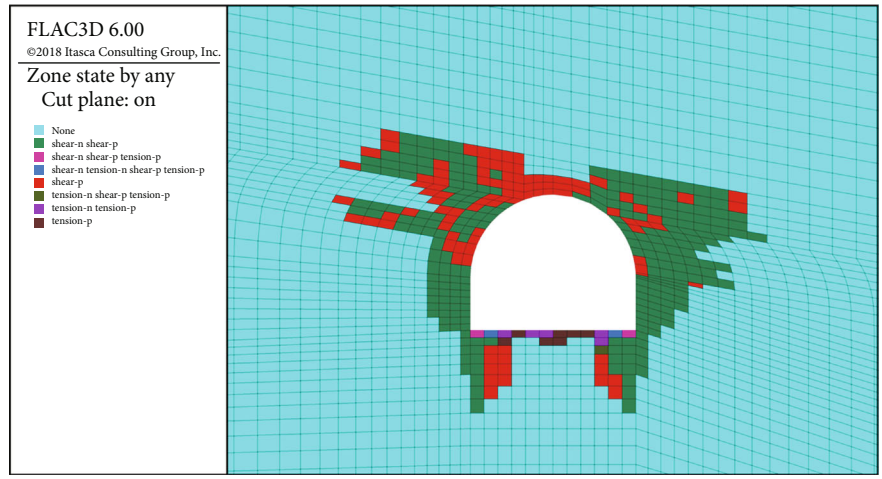

(a) Plastic zone distribution of the original scheme

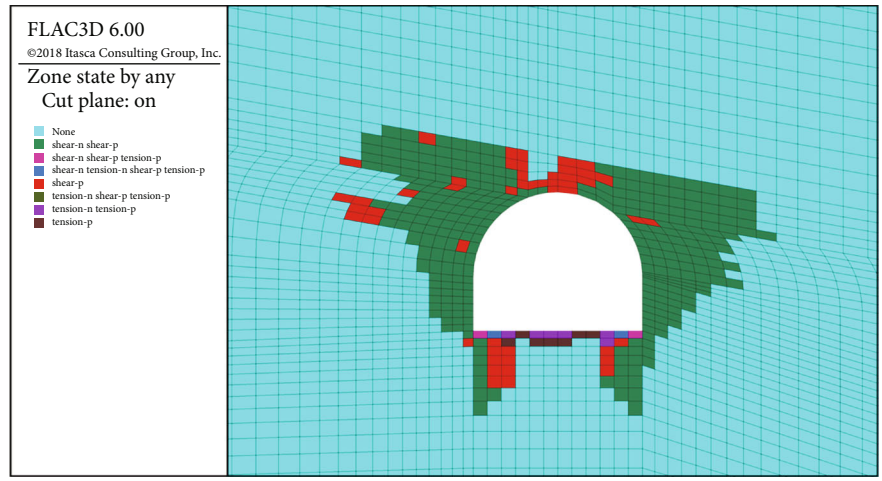

(b) Plastic zone distribution of the ACC support scheme

Figure 10: Distribution diagram of the plastic zone.

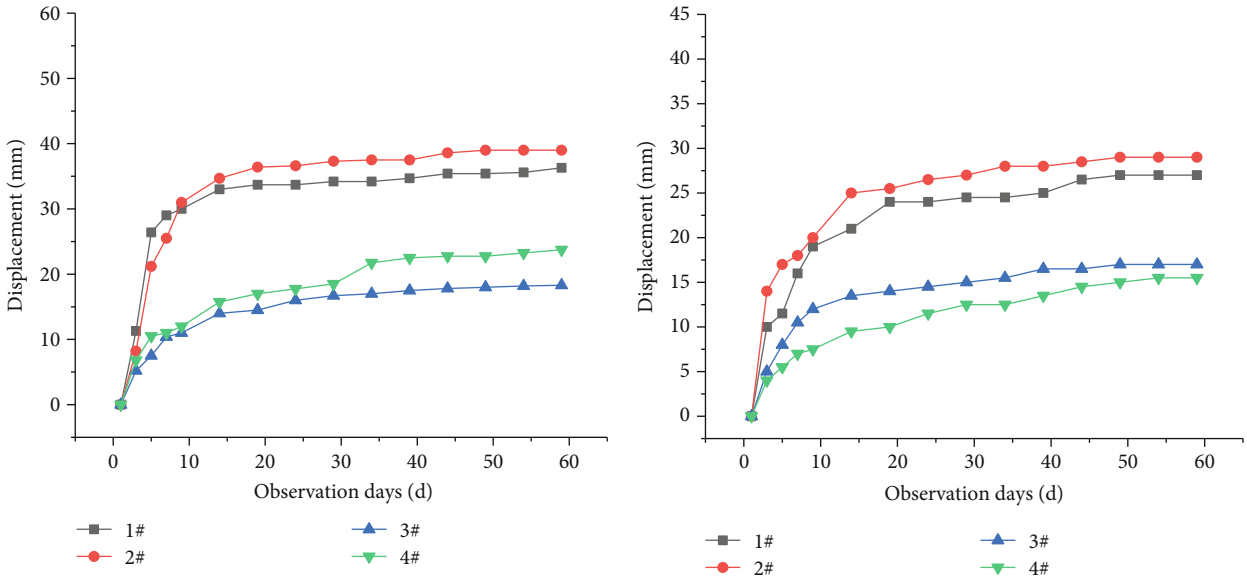

(a) Displacement of the roof and floor

(b) Displacement of the two sides

Figure 11: Field monitoring data.

dimensional stress state to be restored soon after excavation, reducing the plastic deformation range.

5.2. Plastic Zone Analysis. The plastic zone distributions of the original scheme and ACC support scheme are shown in Figure 10.

No significant plastic deformation of the roof occurs in either scheme, which is related to the simulated working conditions of the roadway, where the roadway roof is near the hard rock, and the anchor bolts and anchor cables at the roof and shoulder in both schemes can anchor the fractured rock to the harder roof rock. The plastic zone is clearly distributed along the layers, with the boundary of the plastic zone on the roof being the interface between the coal layer and the sandy mudstone layer as well as the undamaged zone on the left shoulder being the mudstone layer. The plastic zone in the ACC support scheme is significantly smaller in the top and shoulder than that in the original scheme, indicating that the extruded arch formed by the high pretightening anchor cables and concrete spry layer can effectively restore the three-dimensional stress state of the surrounding rock after excavation and control the plastic failure range of the surrounding rock.

6. Field Tests and Analysis of Effects

To test the effectiveness of the full-section ACC support scheme, a field test was carried out in a 200 m long section of the tunnel. During construction, the surface displacement changes within 60 d of excavation were monitored using measuring stations and compared with the deformation of the surrounding rock in the original section. A total of four stations were arranged, numbered 1, 2, 3, and 4. Two stations were arranged in the ACC scheme test section and the original scheme section at 15 m and 30 m from the start of the new scheme, respectively (Figure 11).

Figure 12: Image of the ACC support scheme eight months after tunnel construction.

Monitoring results show that the roadway deformation converged rapidly at the beginning of the support period (within 15 d) and stabilized after 40 d. The average displacement of the roof and floor in the ACC support scheme reached 21 mm, and the average displacement of the two sides reached 16 mm, which were 44.2% and 42.8% less than the original scheme.

There are few differences in the deformation between the roof and floor and between the two sides, indicating that the surrounding rock within the loose zone is better coupled with the ACC support structure, the stress concentration is significantly reduced, surrounding rock stress field area tends to be even, and the resulting displacement field also tends to be even.

The straight wall semicircular arch section of the roadway within 200 m of the ACC test section showed no significant deformation and no anchor cable failures (Figure 12). Field

tests showed that the surface protection structure formed by the reinforcement mesh and concrete spray layer prevented the fractured surrounding rock from falling out and together with the high pretightening force and greater prestress distribution of the ACC ensured the integrity of the extruded arch.

7. Conclusion

A high shear capacity, high pretightening force ACC was developed based on existing anchor cables, and a full-section ACC support system was constructed based on the shear load distribution characteristics of deep roadways and extruded arch theory. Based on borehole peeping and in situ rock stress test results, a full-section ACC support scheme for the tape tunnel was proposed. Numerical simulations and field tests proved that the full-section ACC support scheme effectively controlled crushing and swelling loads within the loose zone and resisted interlayer shear forces. The following conclusions were drawn:

(1) When the free end of the ACC is subjected to lateral shear, the C-shaped tube is gradually compressed and deformed until the free end of the anchor cable is wrapped, enhancing the shear resistance of the free end of the anchor cable. Field tests have shown no anchor cable failure, indicating that the C-tube construction of the ACC significantly increases the shear strength of the free end of the anchor cable. The ACC can resist shear loads in the deep tunnel as well as the crushing and swelling loads within the loose zone

(2) The extruded arch formed by the highly prestressed ACC, reinforcement mesh, and concrete spray layer can keep the surrounding rock inside the loose zone in a three-way stress state, significantly improving its mechanical properties and reducing the plastic deformation range in the surrounding rock. The surface protection provided by the reinforcement mesh and concrete spray layer can prevent the fractured surrounding rock from extruding and falling out, ensuring the integrity of the extruded arch

(3) The traditional combined support methods of anchor bolts, anchor cables, and reinforcement mesh have the disadvantages of insufficient prestressing force and easy shearing off the anchor cables due to large loose zone and shear loads in deep roadways, resulting in large roadway deformations. Compared with the original support scheme, field tests showed that for the ACC support scheme, the deformation between the roof and floor and between the two sides was reduced by 44.2% and 42.8%. The extruded arch structure formed by the ACC, reinforcement mesh, and concrete spray layer is well coupled with the surrounding rock and can effectively control roadway deformation within the loose zone

Data Availability

The data used to support the findings of this study are included within the article.

Conflicts of Interest

The authors declare that they have no conflicts of interest.

Acknowledgments

This paper was supported by the Natural Science Foundation of China (no. 51474218).

References

[1] R. S. Yang, Y. L. Li, M. S. Wang et al., "Experimental study on shear mechanical properties of prestressed anchor cables," *Journal of China University of Mining and Technology*, vol. 47, no. 6, pp. 1166–1174, 2008.

[2] Y. L. Li, *Deformation and Instability Mechanism and Control Technology of Layered Roof in Large Section Coal Roadway of Zhaozhuang Mine*, China University of Mining and Technology, Beijing, 2017.

[3] L. Wang, Q. Wang, Y. B. Huang et al., "Research on deformation mechanism and support technology of deep high-stress tunneling," *Journal of Mining and Safety Engineering*, vol. 36, no. 1, pp. 112–121, 2019.

[4] C. L. Sun, K. Gao, G. J. Cui, and Y. T. Sun, "Stress distribution and asymmetric deformation law of seam entry in inclined deep well," *Coal Mine Safety*, vol. 48, no. 10, pp. 61–64, 2017.

[5] X. Li, G. Yang, J. Nemcik, A. Mirzaghorbanali, and N. Aziz, "Numerical investigation of the shear behaviour of a cable bolt in single shear test," *Tunnelling and Underground Space Technology*, vol. 84, pp. 227–236, 2019.

[6] H. P. Kang, J. H. Yang, F. Q. Gao, and J. Li, "Experimental study on the mechanical behavior of rock bolts subjected to complex static and dynamic loads," *Rock Mechanics and Rock Engineering*, vol. 53, pp. 4993–5004, 2020.

[7] Y. Wu, F. Gao, J. Chen, and J. He, "Experimental study on the performance of rock bolts in coal burst-prone mines," *Rock Mechanics and Rock Engineering*, vol. 52, no. 10, pp. 3959–3970, 2019.

[8] Y. Chen, J. Teng, R. A. Sadiq, and K. Zhang, "Experimental study of bolt-anchoring mechanism for bedded rock mass," *International Journal of Geomechanics*, vol. 20, no. 4, article 04020019, 2020.

[9] H. Lin, Y. Zhu, J. Yang, and Z. Wen, "Anchor stress and deformation of the bolted joint under shearing," *Advances in Civil Engineering*, vol. 2020, no. 6, Article ID 3696489, pp. 1–10, 2020.

[10] K. Spang and P. Egger, "Action of fully-grouted bolts in jointed rock and factors of influence," *Rock Mechanics and Rock Engineering*, vol. 23, no. 3, pp. 201–229, 1990.

[11] W. Q. Chen, Z. X. Jia, Y. F. Zhao, L. P. Liu, J. J. Zhou, and X. C. Lin, "Analysis of axial and transverse action of bolt during shearing," *Rock and Soil Mechanics*, vol. 36, no. 1, pp. 143–148, 2015.

[12] X. G. Zhao, M. F. Cai, M. Cai, and P. Jia, "Interaction between rock dilatancy and bolt support in underground engineering," *Journal of Rock Mechanics and Engineering.*, vol. 29, no. 10, pp. 2056–2062, 2010.

[13] W. Zhang and Q. S. Liu, "Analysis of deformation performance of prestressed bolt based on shear test," *Rock and Soil Mechanics*, vol. 35, no. 8, pp. 2231–2240, 2014.

[14] A. M. Ferrero, "The shear strength of reinforced rock joints," *International Journal of Rock Mechanics and Mining Sciences & Geomechanics Abstracts*, vol. 32, no. 6, pp. 595–605, 1995.

[15] N. Aziz, H. Rasekh, A. Mirzaghorbanali, G. Yang, S. Khaleghparast, and J. Nemcik, "An experimental study on the shear performance of fully encapsulated cable bolts in single shear test," *Rock Mechanics and Rock Engineering*, vol. 51, no. 7, pp. 2207–2221, 2018.

[16] A. Q. Liu, W. J. Ju, H. T. Xu, and Y. Wang, "Experimental study on the influence of anchor bolt pretension on shear performance of jointed rock mass," *Acta Coal Science*, vol. 38, no. 3, pp. 391–396, 2013.

[17] N. Aziz, J. Hossein, and M. S. Hadi, "The effect of rock strength on shear behavior of fully grouted bolts," in *Proceedings Fifth International Symposium on Ground Support in Mining and Underground Construction*, vol. 3, pp. 243–251, Perth, 2004.

[18] N. Aziz, H. Jalalifar, and J. Concalves, "Bolt surface configurations and load transfer mechanism," in *Coal Operators' Conference*, Wollongong, NSW, 2006.

[19] P. F. Jiang, "Study on the evolution of the comprehensive stress field of surrounding rock in mining and roadway excavation in deep extra-thick coal seam," *Coal Science and Technology*, vol. 48, no. 8, pp. 26–36, 2020.

[20] H. W. Jing, Q. B. Meng, J. F. Zhu, B. Meng, and L. Y. Wei, "Stability control theory and technology of deep roadway surrounding rock loosen zone," *Journal of Mining and Safety Engineering*, vol. 37, no. 3, pp. 429–442, 2020.

[21] Y. L. Wang and L. J. Fan, "Research on the differences between traditional suspension, composite arch theory and loosen zone theory," *Science and Technology Vision*, vol. 24, pp. 136-137, 2015.

[22] N. Zhang, B. Y. Li, G. C. Li, D. Y. Qian, and X. Y. Yu, "Uneven failure and closed support of roadway in layers coal and rock mass," *Journal of Mining and Safety Engineering*, vol. 30, no. 1, pp. 1–6, 2013.

[23] R. L. Shan, Y. H. Peng, X. S. Kong et al., "Research progress of coal tunnel support technology at home and abroad," *Chinese Journal of Rock Mechanics and Engineering*, vol. 38, no. 12, pp. 2377–2403, 2019.

[24] R. L. Shan, Y. H. Peng, X. S. Kong, and B. Huang, *Anchor Cable and C-Shaped Tube Structure That can Bear Transverse Shear Force*, CN103967509A, Beijing, 2014.

[25] X. Li, N. Aziz, A. Mirzaghorbanali, and J. Nemcik, "Behavior of fiber glass bolts, rock bolts and cable bolts in shear," *Rock Mechanics and Rock Engineering*, vol. 49, no. 7, pp. 2723–2735, 2016.

[26] M. F. Cai, Q. F. Guo, Y. Li, Z. F. Du, and J. H. Liu, "Ground stress measurement and its application in pingmei no.10 mine," *Journal of University of Science and Technology Beijing*, vol. 35, no. 11, pp. 1399–1406, 2013.